V International Conference on Adaptive Modeling and Simulation
ADMOS 2011
D. Aubry and P. Díez (Eds)

APPPLICATION OF ANISOTROPIC GOAL-ORIENTED UNSTEADY MESH ADAPTATION TO AERODYNAMICS AND AEROACOUSTICS

ANCA C. BELME*, FREDERIC ALAUZET† AND ALAIN DERVIEUX*

*National Institut of Research in Informatics and Automatics (INRIA Sophia-Antipolis)
2004 route des Lucioles
06902 Sophia-Antipolis, France
e-mail: Anca.Belme@inria.fr, Alain.Dervieux@inria.fr
web page: http://www-sop.inria.fr/tropics

†National Institut of Research in Informatics and Automatics (INRIA Rocquencourt)
Domaine de Voluceau
78153 Rocquencourt, France
e-mail: Frederic.Alauzet@inria.fr
web page: http://www-roc.inria.fr/gamma

Key words: A priori error estimate, Anisotropic Adaptation, Goal-Oriented, Adjoint, Continuous Metric

Abstract. The proposed results are in the line of the fully anisotropic goal-oriented mesh adaptation method of Loseille et al.[1]. We consider here the extension to unsteady case. A global fixed-point algorithm is introduced for solving the coupling mesh-solution. Because state is solved forward in time and the adjoint associated to the output functional needs to be solved backwards, a strategy of storage-recomputation is applied. Applications to the emission and reception of sonic and blast waves are presented. The results shows that only the precise part of the wave received by the captor (defining the goal) is followed by the adaptive mesh.

1 INTRODUCTION

Engineering problems commonly require computational fluid dynamics (CFD) solutions with functional outputs of specified accuracy. The computational resources available for these solutions are often limited and errors in solutions and outputs are often unknown. CFD solutions may be computed with an unnecessarily large number of grid points (and associated high cost) to ensure that the outputs are computed to within a required accuracy. One of the powerful methods for increasing the accuracy and reducing the complexity is the mesh adaptation, whose purpose is to control the accuracy of the

numerical solution by changing the discretization of the computational domain according to mesh size and mesh directions constraints.
The technique adopted in this work is the anisotropic mesh adaptation for unsteady flows introduced by Alauzet et al. in [8] combined with a goal-oriented mesh adaptation method.
Starting from a priori estimates, Loseille et al. proposed in [21] a fully anisotropic goal-oriented mesh adaptation technique for steady compressible Euler flows. Extension of this method to unsteady flows is propsed in this paper. First section of this paper is dedicated to a numerical description of the problem for unsteady Euler equations. Then, we introduce the unsteady adjoint system among with its solver. The third part of this paper describes the goal-oriented a priori estimate for the unsteady model. Next, we will present the global transient fixed point algorithm necessary to converge the couple mesh-solution, and finally applications to acoustic waves propagation and blast waves will conclude the present paper.

2 Unsteady Euler model

The unsteady Euler equations for a calorically perfect gas, can be written in a compact variational formulation in the functional space $W \in V = [H^1(\Omega)]^5$ as follows:

$$\forall \phi \in V, \quad (\Psi(W)\,,\,\phi) = \int_\Omega \phi W_t \,\mathrm{d}\Omega + \int_\Omega \phi\, \nabla.\mathcal{F}(W)\,\mathrm{d}\Omega - \int_\Gamma \phi\, \hat{\mathcal{F}}(W).\mathbf{n}\,\mathrm{d}\Gamma \;=\; 0\;, \qquad (1)$$

where by $\Omega \subset R^3$ we denoted the computational domain and Γ its boundary, $\mathbf{n}$ the outward normal to Γ and the boundary flux $\hat{\mathcal{F}}$ contains the different boundary conditions, which involve inflow, outflow and slip boundary conditions.

As a spatially semi-discrete model, we consider the Mixed-Element-Volume formulation [2]. As in [1] we reformulate it under the form of a finite element variational formulation, this time in the unsteady context. We assume that Ω is covered by a finite-element partition in simplicial elements K. The mesh is the set of K's, denoted by $\mathcal{H}$. Let us introduce the following approximation space:

$$V_h \;=\; \left\{\phi_h \in V \cap \mathcal{C}^0(\bar{\Omega}) \;\middle|\; \phi_{h|K} \text{ is affine } \forall K \in \mathcal{H}\right\}.$$

and the interpolation operator is chosen as the usual $\mathcal{P}^1$ operator:

$$\Pi_h :\; V \cap \mathcal{C}^0(\bar{\Omega}) \rightarrow\; V_h \;\text{ such that }\; \Pi_h\varphi(\mathbf{x}_i) = \varphi(\mathbf{x}_i),$$

for all vertices $\mathbf{x}_i$ of $\mathcal{H}$.
We extend it to time-dependent functions:

$$\Pi_h :\; H^1\{[0,T];V\} \rightarrow\; \mathcal{V}_h \;\text{ such that }\; (\Pi_h\varphi)\,(t) = \Pi_h\,(\varphi(t))\,,\; \forall\; t \in\; [0,T].$$

The weak discrete formulation writes:

$$\forall \phi_h \in V_h,\; (\Psi_h(W_h)\,,\,\phi_h) = 0,$$

with

$$\begin{aligned}(\Psi_h(W_h)\,,\,\phi_h) &= \int_{\Omega_h} \phi_h W_{h,t}\,\mathrm{d}\Omega_h + \int_{\Omega_h} \phi_h \nabla.\mathcal{F}_h(W_h)\,\mathrm{d}\Omega_h \\ &- \int_{\Gamma_h} \phi_h \hat{\mathcal{F}}_h(W_h).\mathbf{n}\,\mathrm{d}\Gamma_h + \int_{\Omega_h} \phi_h\, D_h(W_h)\mathrm{d}\Omega_h\end{aligned} \tag{2}$$

with $\mathcal{F}_h = \Pi_h \mathcal{F}$ and $\hat{\mathcal{F}}_h = \Pi_h \hat{\mathcal{F}}$ and $\Gamma_h = \partial\Omega_h$. The numerical diffusion term D_h is at least a third order term with respect to mesh size, everywhere limiters do not apply. Even for shocked flows, we have found it is interesting to neglect it, see [1]. This option is also followed in this paper.
As for time advancing, an explicit scheme is considered, more preciselly, a Strong-Stability-Preserving (SSP) Runge-Kutta scheme. Such time discretization methods have non-linear stability properties like TVD which are particularly suitable for the integration of system of hyperbolic conservation laws where discontinuities appear.

3 Error Analysis

For a solution W of state system (1), we define the *functional output* as:

$$j \in \mathbb{R}\ ;\ j = (g, W). \tag{3}$$

The *continuous adjoint* W^* is the solution of:

$$W^* \in \mathcal{V}\ ,\ \forall \psi \in \mathcal{V}\ ,\ \left(\frac{\partial \Psi}{\partial W}(W)\psi, W^*\right) = (g, \psi)\ . \tag{4}$$

The objective is to estimate the following approximation error on the functional:

$$\delta j = j(W) - j(W_h)\ ,$$

where W and W_h are respectively solutions of (1) and (2). Using the fact that $\mathcal{V}_h \subset \mathcal{V}$, the following error estimates for the unknown can be written:

$$(\Psi_h(W), \varphi_h) - (\Psi_h(W_h), \varphi_h) = (\Psi_h(W), \varphi_h) - (\Psi(W), \varphi_h) = ((\Psi_h - \Psi)(W), \varphi_h). \tag{5}$$

It is then useful to choose the test function φ_h as the discrete adjoint state, $\varphi_h = W_h^*$, which is the solution of:

$$\forall \zeta_h \in \mathcal{V}_h,\ \left(\frac{\partial \Psi_h}{\partial W_h}(W_h)\zeta_h\,,\, W_h^*\right) = (g, \zeta_h), \tag{6}$$

We assume that W_h^* is close to the continuous adjoint state W^*. We refer to [1] in which the following *a priori* formal estimate is finally proposed:

$$\delta j \approx ((\Psi_h - \Psi)(W), W^*)\ . \tag{7}$$

Application to unsteady compressible Euler: We replace in estimator (7) operators Ψ and Ψ_h by their expressions given by relations (1) and (2) . In [1], it was observed that even for shocked flows, it is interesting to neglect the D_h numerical viscosity term. We follow again here this option. We also discard the error term due to the imposition of the initial condition. After integrating by parts we get:

$$\begin{aligned}\delta j &\approx \int_0^T \int_\Omega W^* \left(W - \Pi_h W\right)_t \,\mathrm{d}\Omega\; dt \\ &- \int_0^T \int_\Omega \nabla W^* \left(\mathcal{F}(W) - \Pi_h \mathcal{F}(W)\right) \mathrm{d}\Omega\; dt \\ &- \int_0^T \int_\Gamma W^* \left(\bar{\mathcal{F}}(W) - \Pi_h \bar{\mathcal{F}}(W)\right)\right).\mathbf{n}\,\mathrm{d}\Gamma\; dt. \end{aligned} \tag{8}$$

with $\bar{\mathcal{F}} = \hat{\mathcal{F}} - \mathcal{F}$. We observe that this estimate of δj is expressed in terms of interpolation errors of the Euler fluxes and of the time derivative weighted by continuous functions W^* and ∇W^*.

Error bound with a safety principle. The integrands in error estimator (8) contain positive and negative parts which can compensate for some particular meshes. In our strategy, we prefer not to rely on these parasitic effects and to slightly over-estimate the error. To this end, all integrands are bounded by their absolute values:

$$\begin{aligned}(g, W_h - W) \leq &\int_0^T \int_\Omega |W^*|\,|\left(W - \Pi_h W\right)_t|\,\mathrm{d}\Omega\; dt \\ &+ \int_0^T \int_\Omega |\nabla W^*|\,|\mathcal{F}(W) - \Pi_h \mathcal{F}(W)|\,d\Omega\; dt \\ &+ \int_0^T \int_\Gamma |W^*|\,|(\bar{\mathcal{F}}(W) - \Pi_h \bar{\mathcal{F}}(W)).\mathbf{n}|\,d\Gamma\; dt. \end{aligned} \tag{9}$$

4 Optimal metric

We propose to work in a continuous mesh framework, which is made easier thanks to the *a priori* estimate. It allows us to define proper differentiable optimization [3, 4] or to use the calculus of variations that is undefined on the class of discrete meshes. This framework lies in the class of metric-based methods.

4.1 Continuous mesh model

A continuous mesh $\mathbf{M} = (\mathcal{M}(\mathbf{x}))_{\mathbf{x}\in\Omega}$ of Ω is a Riemannian metric field [5]. For all $\mathbf{x}$ of Ω, $\mathcal{M}(\mathbf{x})$ is a symmetric tensor having $(\lambda_i(\mathbf{x}))_{i=1,3}$ as eigenvalues along the principal directions $\mathcal{R}(\mathbf{x}) = (\mathbf{v}_i(\mathbf{x}))_{i=1,3}$. Sizes along these directions are denoted $(h_i(\mathbf{x}))_{i=1,3} =$

$(\lambda_i^{-\frac{1}{2}}(\mathbf{x}))_{i=1,3}$. With this definition, $\mathbf{M}$ admits the more practical local decomposition:

$$\mathcal{M}(\mathbf{x}) = d^{\frac{2}{3}}(\mathbf{x})\,\mathcal{R}(\mathbf{x}) \begin{pmatrix} r_1^{-\frac{2}{3}}(\mathbf{x}) & & \\ & r_2^{-\frac{2}{3}}(\mathbf{x}) & \\ & & r_3^{-\frac{2}{3}}(\mathbf{x}) \end{pmatrix} {}^t\mathcal{R}(\mathbf{x}),$$

where

- the node density d is equal to: $d = (h_1 h_2 h_3)^{-1} = (\lambda_1\lambda_2\lambda_3)^{\frac{1}{2}} = \sqrt{\det(\mathcal{M})}$,
- the three anisotropic quotients r_i are equal to: $r_i = h_i^3\,(h_1 h_2 h_3)^{-1}$.

By integrating the node density, we define the complexity $\mathcal{C}$ of a continuous mesh which is the continuous counterpart of the total number of vertices:

$$\mathcal{C}(\mathbf{M}) = \int_\Omega d(\mathbf{x})\,d\mathbf{x} = \int_\Omega \sqrt{\det(\mathcal{M}(\mathbf{x}))}\,d\mathbf{x}.$$

Given a continuous mesh $\mathbf{M}$, we shall say, following [**?**], that a discrete mesh $\mathcal{H}$ of the same domain Ω is a **unit mesh with respect to M**, if each tetrahedron $K \in \mathcal{H}$, defined by its list of edges $(\mathbf{e}_i)_{i=1\ldots6}$, verifies:

$$\forall i \in [1,6], \quad \ell_{\mathcal{M}}(\mathbf{e}_i) \in \left[\frac{1}{\sqrt{2}}, \sqrt{2}\right] \quad \text{and} \quad Q_{\mathcal{M}}(K) \in [\alpha, 1] \;\text{ with }\; \alpha > 0\,,$$

in which the length of an edge $\ell_{\mathcal{M}}(\mathbf{e}_i)$ and the quality of an element $Q_{\mathcal{M}}(K)$ are defined as follows:

$$Q_{\mathcal{M}}(K) = \frac{36}{3^{\frac{1}{3}}} \frac{|K|_{\mathcal{M}}^{\frac{2}{3}}}{\sum_{i=1}^{6} \ell_{\mathcal{M}}^2(\mathbf{e}_i)} \in [0,1], \;\text{ with } |K|_{\mathcal{M}} = \int_K \sqrt{\det(\mathcal{M}(\mathbf{x}))}\,\mathrm{d}\mathbf{x},$$
$$\text{and } \ell_{\mathcal{M}}(\mathbf{e}_i) = \int_0^1 \sqrt{{}^t\mathbf{ab}\;\mathcal{M}(\mathbf{a}+t\,\mathbf{ab})\;\mathbf{ab}}\;\mathrm{d}t, \quad \text{with } \mathbf{e}_i = \mathbf{ab}.$$

We choose a tolerance α equal to 0.8.
Given a smooth function u, to each unit mesh $\mathcal{H}$ corresponds a local interpolation error $|u - \Pi u|$. In [**?**] it is shown that all these interpolation errors are well represented by the so-called continuous interpolation error related to $\mathcal{M}$, which is expressed in terms of the Hessian H_u of u as follows:

$$\begin{aligned}(u - \pi_{\mathcal{M}} u)(\mathbf{x},t) &= \frac{1}{10}\mathrm{trace}(\mathcal{M}^{-\frac{1}{2}}(\mathbf{x})\,|H_u(\mathbf{x},t)|\,\mathcal{M}^{-\frac{1}{2}}(\mathbf{x})) \\ &= \frac{1}{10} d(\mathbf{x})^{-\frac{2}{3}} \sum_{i=1}^{3} r_i(\mathbf{x})^{\frac{2}{3}}\,{}^t\mathbf{v_i}(\mathbf{x})\,|H_u(\mathbf{x},t)|\,\mathbf{v_i}(\mathbf{x}), \qquad (10)\end{aligned}$$

where $|H_u|$ is deduced from H_u by taking the absolute values of its eigenvalues and where time-dependency notations have been added for use in next sections.

4.2 Error model minimization

Working in this framework enables us to write Estimate (9) in a continuous form:

$$
\begin{aligned}
|(g, W_h - W)| \approx E(\mathbf{M}) \;\; = \;\; & \int_0^T \int_\Omega |W^*| \;\; |\big(W - \pi_{\mathcal{M}} W\big)_t| \, \mathrm{d}\Omega \; dt \\
& + \int_0^T \int_\Omega |\nabla W^*| \;\; |\mathcal{F}(W) - \pi_{\mathcal{M}} \mathcal{F}(W)| \, d\Omega \; dt \\
& + \int_0^T \int_\Gamma |W^*| \;\; |(\bar{\mathcal{F}}(W) - \pi_{\mathcal{M}} \bar{\mathcal{F}}(W)).\mathbf{n}| \, d\Gamma \; dt, \qquad (11)
\end{aligned}
$$

where $\mathbf{M} = (\mathcal{M}(\mathbf{x}))_{\mathbf{x}\in\Omega}$ is a continuous mesh defined by a Riemannian metric space and $\pi_{\mathcal{M}}$ is the continuous linear interpolate defined hereafter. In the general case, we need to split the description of the mesh into the volumic mesh, described by $\mathbf{M}$ and the surfacic mesh for the boundary, described by $\bar{\mathbf{M}}$. The error dependancy to these two meshes writes:

$$
E(\mathbf{M}, \bar{\mathbf{M}}) = \sum_k \int_0^T \int_\Omega g_k |(1 - \pi_{\mathcal{M}}) u_k| \mathrm{d}\Omega \; dt + \sum_k \int_0^T \int_\Gamma \bar{g}_k |(1 - \pi_{\bar{\mathcal{M}}}) \bar{u}_k| d\Gamma \; dt \; . \qquad (12)
$$

In the different couples (g_k, u_k), we account for all the integrands in the volumic integral, that is the term from the time derivative, and the 15 terms resulting from the multiplication of interpolation error of Euler fluxes by adjoint spatial derivatives.
In the different couples $(\bar{g}_k, \bar{u}_k)$, are accounted the five terms resulting from the multiplication of interpolation error of boundary Euler fluxes by adjoint components, this for all time levels.
Before solving the minimisation system, we simplify it a little more. Indeed, when minimising $E(\mathbf{M}, \bar{\mathbf{M}})$ with respect to $\mathbf{M}$ and $\bar{\mathbf{M}}$, we manage to adapt simultaneously the volumic mesh and the mesh of its boundary. We would like to emphasise that the optimal surface mesh is generally not the trace of the optimal volumic mesh. The fully anisotropic goal-oriented mesh adaptation formulation carries informations for improving the surface mesh. In [**?**], an analysis including the boundary mesh is proposed. In many cases, it is enough to optimise the volumic mesh. Choosing that latter case, we discard the $\bar{\mathbf{M}}$ component and related integrals:

$$
\text{Find } \mathbf{M}_{opt} = \text{Argmin}_{\mathbf{M}} \, E(\mathbf{M}), \qquad (13)
$$

under the constraint of bounded mesh fineness:

$$
\mathcal{C}_{\text{st}}(\mathbf{M}) = N. \qquad (14)
$$

where N is a specified total number of nodes. Since we consider an unsteady problem, the space-time (st) cost in computing the solution needs now to take into account the time

discretisation. The above constraint then imposes the total number of nodes in the time integral, that is:

$$\mathcal{C}_{\mathrm{st}}(\mathbf{M}) = \int_0^T \tau(t)^{-1}\mathrm{d}t \int_\Omega d_{\mathcal{M}}(\mathbf{x})\mathrm{d}x$$

where $\tau(t)$ is the time step used at a time t of interval $]0,T[$.

4.3 Optimal goal-oriented metric

For each vertex $\mathbf{x}$ of Ω, a 3×3 symmetric matrix arising from the volume contribution of the sum of the Hessian of each component of the Euler fluxes weighted by the gradient of the adjoint state and the Hessian of the state time derivative weighted by the adjoint state:

$$E(\mathbf{M}) = \int_\Omega |\frac{1}{10}\mathrm{trace}(\mathcal{M}^{-\frac{1}{2}}(\mathbf{x})\,|\mathbf{H}(\mathbf{x})|\,\mathcal{M}^{-\frac{1}{2}}(\mathbf{x}))|\mathrm{d}\Omega$$

$$\mathbf{H}(\mathbf{x}) = \sum_{n=1}^{m}\sum_{j=1}^{5}\left([\Delta t]_j(\mathbf{x}) + [\Delta x]_j(\mathbf{x}) + [\Delta y]_j(\mathbf{x}) + [\Delta z]_j(\mathbf{x})\right), \tag{15}$$

where

$$\begin{aligned}
[\Delta t]_j(\mathbf{x}) &= \int_0^T \left|W_j^*(\mathbf{x},t)\right| \cdot \left|H((W_{j,t}))(\mathbf{x},t)\right|\, dt,\\
[\Delta x]_j(\mathbf{x}) &= \int_0^T \left|\frac{\partial W_j^*}{\partial x}(\mathbf{x},t)\right| \cdot \left|H(\mathcal{F}_1(W_j))(\mathbf{x},t)\right|\, dt,\\
[\Delta y]_j(\mathbf{x}) &= \int_0^T \left|\frac{\partial W_j^*}{\partial y}(\mathbf{x},t)\right| \cdot \left|H(\mathcal{F}_2(W_j))(\mathbf{x},t)\right|\, dt,\\
[\Delta z]_j(\mathbf{x}) &= \int_0^T \left|\frac{\partial W_j^*}{\partial z}(\mathbf{x},t)\right| \cdot \left|H(\mathcal{F}_3(W_j))(\mathbf{x},t)\right|\, dt\ .
\end{aligned}$$

with W_j^* denoting the j^{th} component of the adjoint vector W^* and $H(\mathcal{F}_i(W_j))$ the Hessian of the j^{th} component of the vector $\mathcal{F}_i(W)$, The solution of the error optimisation problem (13,14) is the optimal metric goal oriented ("*go*") tensor field:

$$\mathcal{M}_{go}(\mathbf{x}) = C\ \det(|\mathbf{H}(\mathbf{x})|)^{-\frac{1}{5}}|\mathbf{H}(\mathbf{x})|, \tag{16}$$

where constant C depends on the desired space-time complexity N. In the simplest case where the time step $\tau(t)$ used at time t does not depend on the adapted spatial mesh, then the value of C is easily found as:

$$C \;=\; \left(\frac{N}{\int_0^T(\tau(t))^{-1}\mathrm{d}t}\right)^{\frac{2}{3}}\left(\int_\Omega \det(|\mathbf{H}(\mathbf{x})|)^{\frac{1}{5}}\right)^{\frac{2}{3}}. \tag{17}$$

In the case of an explicit time advancing we get a more complex context, since time step strongly depends on the smallest mesh size. A model need be chosen for this dependence and accounted for finding C. Once C is obtained, we can make explicit the minimal value of the error functional which will be in the simplest above case:

$$\mathbf{E}(\mathbf{M}_{go}) = N^{\frac{2}{3}} \left(\int_\Omega det(|\mathbf{H}(\mathbf{x})|)^{\frac{1}{5}} \right)^{\frac{5}{3}}. \tag{18}$$

Continuous problem (13) has been solved from an explicit optimality condition producing the optimal metric field as a function of continuous state and adjoint. This means that the coupled mesh optimality continuous system writes:

$$\begin{aligned} &W \in \mathcal{V}\ ,\ \forall \varphi \in \mathcal{V}\ ,\ \ (\Psi(\mathcal{M}, W), \varphi) = 0 && \text{“Euler”} \\ &W^* \in \mathcal{V}\ ,\ \forall \psi \in \mathcal{V}\ ,\ \ \left(\frac{\partial \Psi}{\partial W}(\mathcal{M}, W)\psi, W^* \right) = (g, \psi) && \text{“adjoint”} \\ &\mathcal{M}(\mathbf{x}) = \left(\frac{N \int_\Omega \det(|\mathbf{H}(W, W^*, \mathbf{x})|)^{\frac{1}{5}}}{\int_0^T (\tau(t))^{-1} \mathrm{d}t} \right)^{\frac{2}{3}} \det(|\mathbf{H}(W, W^*, \mathbf{x})|)^{-\frac{1}{5}} |\mathbf{H}(W, W^*, \mathbf{x})|. && (19) \end{aligned}$$

In practice, it remains to approximate the above three-field coupled system by a discrete one. For discretising the state and adjoint PDE's, we take the spatial schemes introduced below and the explicit Runge-Kutta time advancing schemes. Discretising the last equation consists in specifying the mesh according to a discrete metric deduced from the discrete states.

5 Unsteady Adjoint state and Lagrange multipliers

Consider the following semi-discrete unsteady compressible Euler model (RK1):

$$\Psi^n(W^n, W^{n-1}) = \frac{W^n - W^{n-1}}{\delta t^n} + \Phi(W^{n-1}) = 0 \quad \text{for } n = 1, ..., N. \tag{20}$$

The time-dependent functional is discretised as follows:

$$j(W) = \sum_{n=1}^{N} \delta t^n j^{n-1}(W).$$

The problem of minimizing the error committed on the target functional $j(W) = (g, W)$, subject to the Euler system (20), can be transformed into an unconstrained problem for the following Lagrangian functional:

$$\mathcal{L} = \sum_{n=1}^{N} \delta t^n j^{n-1}(W) - \sum_{n=1}^{N} \delta t^n (W^{*,n})^T \Psi^n(W^n, W^{n-1})$$

where $W^{*,n}$ are the N vectors of the Lagrange multipliers (which are the time-dependent adjoint states). The conditions for an extremum becomes then:

$$\frac{\partial \mathcal{L}}{\partial W^{*,n}} = 0 \quad \text{and} \quad \frac{\partial \mathcal{L}}{\partial W^{n}} = 0, \quad \text{for } n = 1, ..., N.$$

The first condition is easily verified using assumption (20). Thus the lagrangien multipliers $W^{*,n}$ must be chosen such that the second condition of extrema $\frac{\partial \mathcal{L}}{\partial W^n} = 0$ is verified. This gives the unsteady discret adjoint system:

$$\left\{ \begin{array}{rcl} W^{*,N} & = & 0 \\ W^{*,n} & = & W^{*,n+1} + \delta t^{n+1} \dfrac{\partial j^n}{\partial W^n} - \delta t^{n+1} (W^{*,n+1})^T \dfrac{\partial \Psi^n}{\partial W^n} \end{array} \right. \tag{21}$$

As the adjoint system runs in reverse time, the first expression in the adjoint system (21) is referred to as adjoint "initialization".

Computing $W^{*,n}$ at time t^n requires the knowledge of state W^n and adjoint state $W^{*,n+1}$. Moreover, the knowledge of all states $\{W^n\}_{n=1,N}$ is needed which involves large memory storage effort. This drawback can be reduced by out-of-core storage of checkpoints (as shown in the picture below), although it implies a recomputing effort of the state W.

5.1 Unsteady mesh adaptation model

To converge the couple mesh-solution, a fixed-point mesh adaptation algorithm has been successfully used in [6]. When an adjoint-based criterion is adopted this algorithm cannot be used efficiently. Thus, similary to [7], we pass to a global fixed point covering the whole time-frame $[0, T]$, and define a *Global adjoint fixed-point mesh adaptation algorithm*:

```
 //--- Fixed-point loop to converge the global space-time mesh adaptation
For j=1,nptfx  //--- Solve state once to get checkpoints
For i=1,n_adap
```

- $\mathcal{S}^j_{0,i} = \texttt{ConservativeSolutionTransfer}(\mathcal{H}^j_{i-1}, \mathcal{S}^j_{i-1}, \mathcal{H}^j_i)$
- $\mathcal{S}^j_i = \texttt{SolveStateForward}(\mathcal{S}^j_{0,i}, \mathcal{H}^j_i)$

```
 End for  //--- Solve state and adjoint backward and store samples
For i=n_adap,1
```

- $(\mathcal{S}^*)^j_i = \texttt{AdjointStateTransfer}(\mathcal{H}^j_{i+1}, (\mathcal{S}^*_0)^j_{i+1}, \mathcal{H}^j_i)$
- $\{\mathcal{S}^j_i(k), (\mathcal{S}^*)^j_i(k)\}_{k=1,n_k} = \texttt{SolveStateAndAdjointBackward}(\mathcal{S}^j_{0,i}, (\mathcal{S}^*)^j_i, \mathcal{H}^j_i)$
- $|\mathbf{H}_{\max}|^j_i = \texttt{ComputeGoalOrientedHessianMetric}(\mathcal{H}^j_i, \{\mathcal{S}^j_i(k), (\mathcal{S}^*)^j_i(k)\}_{k=1,n_k})$

`End for`

- $\mathcal{C}^j$ = `ComputeSpaceTimeComplexity`$(\{|\mathbf{H}_{\max}|_i^j\}_{i=1,n_{adap}})$
- $\{\mathcal{M}_i^j\}_{i=1,n_{adap}}$ = `ComputeUnsteadyGoalOrientedMetrics`$(\mathcal{C}^j, \{|\mathbf{H}_{\max}|_i^j\}_{i=1,n_{adap}})$
- $\{\mathcal{H}_i^{j+1}\}_{i=1,n_{adap}}$ = `GenerateAdaptedMeshes`$(\{\mathcal{H}_i^j\}_{i=1,n_{adap}}, \{\mathcal{M}_i^j\}_{i=1,n_{adap}})$

`End for`

To summarise the algorithm consists in splitting the time interval $[0, T]$ into n_{adap} mesh-adaptation time subintervals. Then, state solution time-forward computation is performed with a storage of the checkpoints. Starting from the last sub-interval (loop $i = n_{adap}, 1$) we solve time-backward for the adjoint.At the same time, we compute metrics $|\mathbf{H}_{\max}|_i^j$ needed to generate new individual meshes per sub-interval. Transfers between two successive solutions/checkpoints are performed by using a conservative transfer (see [?]). This steps are repeated a fixed number of $nptfx$ times (typically $5-15$ global iterations are sufficient).

6 Numerical Experiments

6.1 2D Acoustic wave propagation

We consider a sound source located at the center-bottom of a rectangular domain.

We are interested by the mesh-adaptive calculation of the impact of the sound on a micro **M** located on the center of the same domain top. The role expected from mesh adaptation is to reduce as much as possible mesh fineness in the parts of computational domain where accuracy loss does not influence the quality of sound prediction on the micro. This is illustrated in Figure 1.
The analysis of the integrand $k(t) = \int_M \frac{1}{2}(p - p_{air})^2 \mathrm{d}M$ of $j(W) = \int_0^T k(t)\mathrm{d}t$ on the micro M for different sizes of non-adapted meshes shows, as picturized in Figure 2 (left image), that for a rather coarse mesh of about $60,000$ nodes we have a small perturbation at the entrance of the micro, that diminishes with finer meshes. This behaviour is completeley disolved with the adaptive mesh computation (Figure 2 right image).

Convergence analysis:

For a mesh of N vertices, let us call the approximate solution u_N and u_{exact} the exact solution. The following relation holds:

$$u_N(x,t) \;=\; u_{exact}(x,t) \;+\; N^{-\frac{\alpha}{d}} u_1(x,t) \;+\; o(N^{-\frac{\alpha}{d}})$$

for d spatial dimension, α the convergence parameter to be found and u_1 the first normalized error term. Since α cannot be directly determined, an estimation is done on three meshes of different sizes. Suppose u_{N_1},u_{N_2} and u_{N_3} the corresponding numerical solution

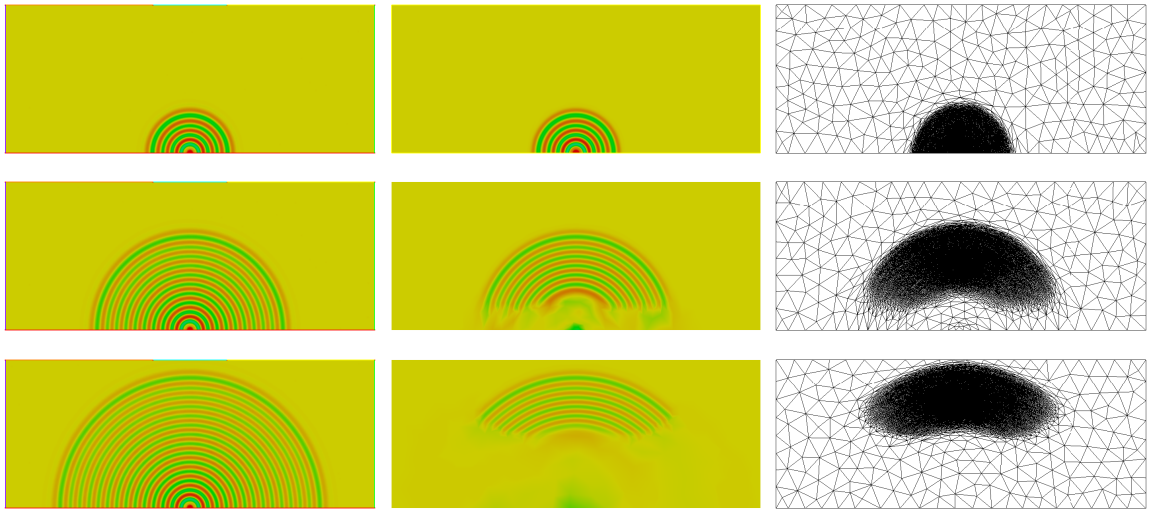

Figure 1: 2D Acoustic Blast wave. Propagation of acoustic waves: density field evolving in time on uniform mesh (left), adapted one (middle), with corresponding images of adaped meshes (right)

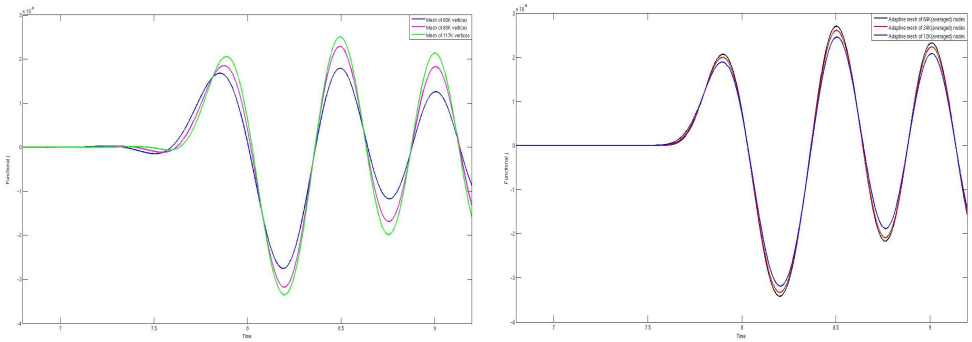

Figure 2: 2D Acoustic Blast wave. Functional time integrand calculation on different sizes of non-adapted meshes(left) vs. adapted ones (right)

computed on different meshes of respectively N_1, N_2 and N_3 number of vertices.

We search for α such that :

$$\frac{1-\frac{N_2}{N_1}^{-\frac{\alpha}{d}}}{1-\frac{N_3}{N_1}^{-\frac{\alpha}{d}}} \approx \frac{u_{N_1}-u_{N_2}}{u_{N_1}-u_{N_3}} \tag{22}$$

with the dimension $d = 2$ in our case.

Furthermore, we make the assumption that N_1 represent the higher number of vertices and N_3 the lowest one.

We solve equation (22) for both uniform and adapted meshes presented in the previous section (see Figure 2). The values of u_{N_i}, with $i = 1, 2, 3$ are considered as the first

Mesh	**First observed maximum**	**Convergence order**
Uniform mesh 60K nodes	$1.67578e-06$	
Uniform mesh 80K nodes	$1.84838e-06$	**0.6**
Uniform mesh 117K nodes	$2.05461e-06$	
Adapted mesh 12K nodes	$1.89061e-06$	
Adapted mesh 24K nodes	$1.99895e-06$	**1.98**
Adapted mesh 64K nodes	$2.06722e-06$	

Table 1: 2D Acoustic Blast wave. Mesh convergence for the time-dependent pressure deviation on observation area

maximal values observed. Tab. 6.1 summarizes the data collection for the three meshes and the convergence order is found to be 0.6 for uniform meshes and 1.98 for the adapted one.

REFERENCES

[1] Loseille, A. and Dervieux, A. and Alauzet, F. Fully anisotropic goal-oriented mesh adaptation for 3D steady Euler equations. *Journal of Computational Physics* (2010) **229**:2866–2897.

[2] Cournède, P.-H., Koobus, B. and Dervieux, A. Positivity statements for a Mixed-Element-Volume scheme on fixed and moving grids. *European Journal of Computational Mechanics* (2006) **15**:767–798

[3] Absil, P.-A., Mahony, R. and Sepulchre, R. *Optimization Algorithms on Matrix Manifolds*. Princeton University Press, (2008).

[4] Arsigny, V., Fillard, P., Pennec, X. and Ayache, N. Log-Euclidean Metrics for Fast and Simple Calculus on Diffusion Tensors. *Magn. Reson. Med.* (2006) **56**:411–421

[5] Berger, M. *A panoramic view of Riemannian geometry*. Springer Verlag, (2003).

[6] Alauzet, F., Frey, P.J., George, P.L. and Mohammadi, B. 3D transient fixed point mesh adaptation for time-dependent problems: Application to CFD simulations. *Journal of Computational Physics* (2007) **222**:592–623

[7] Olivier, G and Alauzet, F. A New Changing-Topology ALE Scheme for Moving Mesh Unsteady Simulations. *49th AIAA Aerospace Sciences Meeting and Exhibit.* (2011)

[8] Alauzet, F. Adaptation de maillage anisotrope en trois dimensions. Application aux simulations instationnaires en Mécanique des Fluides. *Thesys University of Montpellier II.* (2003)